Improved freshwater generation via hemispherical solar desalination unit using paraffin wax as phase change material encapsulated in waste aluminium cans

Thamarai Kannan B[a], B. Madhu[b], AE Kabeel[c,d], Amrit Kumar Thakur[a*], R, Velraj[e], I. Lynch[f], R. Saidur[g,k], Ravishankar Sathyamurthy[a,h,**]

[a] Department of Mechanical Engineering, KPR Institute of Engineering and Technology, Arasur, Coimbatore-641407, Tamil Nadu, India

[b] Department of Mechanical Engineering, Velammal Institute of Technology, Panchetti, Tamil Nadu, India

[c] Mechanical Power Engineering Department, Faculty of Engineering, Tanta University, Egypt

[d] Faculty of Engineering, Delta University for Science and Technology, Egypt.

[e] Institute for Energy Studies, Anna University, Chennai, 600025, Tamil Nadu, India.

[f] School of Geography, Earth and Environmental Sciences, University of Birmingham, Edgbaston, B15 2TT, Birmingham, UK

[g] Research Center for Nano-Materials and Energy Technology (RCNMET), School of Engineering and Technology, Sunway University, Bandar Sunway, Petaling Jaya 47500, Selangor Darul Ehsan, Malaysia

[h] Mechanical Engineering Department, King Fahd University of Petroleum & Minerals, Dhahran, 31261, Saudi Arabia

[k] Department of Engineering, Lancaster University, Lancaster, LA1 4YW, UK

*** Corresponding author** – Amrit Kumar Thakur (amritt1@gmail.com)

**** Corresponding author** - Ravishankar Sathyamurthy (raviannauniv23@gmail.com, ravishankars05@outlook.com, ravishankarsathyamurthy@gmail.com)

Formatted: Font: 12 pt, Not Italic, Superscript

Formatted: Font: 12 pt, Not Italic

Abstract

The present work aims to increase the amount of water generated by the hemispherical solar still (HSS) using paraffin wax as phase change material (PCM) encapsulated in waste aluminium-cans in two different shape of square pattern (4 PCM cans) and triangular pattern (3 PCM cans). Furthermore, a comparative analysis for the conventional HSS over the modified HSS with PCM two different arrangement was carried out to optimize the most suitable mass of PCM. Results showed that PCM encapsulated in aluminium cans in square and triangular patterns placed in HSS basin augmented the clean water production by 92.80% (full day water generation of 5.63 kg/m^2) and 67.12% (full day water generation of 4.88 kg/m^2) respectively, as compared to the bare HSS without any PCM (full day water generation of 2.92 kg/m^2). The effective utilization of the heat from the aluminium cans filled with paraffin wax augmented the potable water production with increased evaporation of water. The economic analysis revealed that with the use of PCM encapsulated cans in square and triangular pattern, the cost per liter of water produced reduced to 67.65% and 45.31% respectively than HSS without any PCM. It was concluded that the low-cost encapsulating material with excellent conductivity and maximum mass of PCM (4 PCM cans in present case) could be beneficial in generating higher amount of freshwater from brackish water.

Keywords: - Fresh water generation; Solar desalination; Hemispherical condenser cover; Paraffin wax; Phase change material; Aluminium encapsulation.

1. Introduction

Desalination is normally a process of removing the contaminants available in the sea / brackish water to make it suitable for drinking purpose. The process has become the most

prominent one in providing clean and potable water across the globe. The recent studies reported that during the early 1950's, an average amount of 4000 m^3 of water / year was consumed by a person which has been drastically reduced to 1000 m^3 / year now that is due to the severe scarcity of the fresh water [1]. Due to rising population and development, the need for fresh water has tremendously increased with time and it requires immediate attention towards development of sustainable clean energy solution for fresh water generation.

Solar process is almost a zero-emission process, and improvements in solar technology have made it possible to overcome previously encountered issues like dust and high temperatures, which reduced the effectiveness of previously utilized solar panels and made them less efficient. Solar stills is the most sustainable water purification device that operates via solar energy, however it has less practical applications owing to the lower overall performance and its dependability on solar energy (which is intermittent in nature) during the operations. As fossil fuel prices are escalating and their usage are possessing a big threat to the environment, researches are focusing on improving the thermal performance of the stills via different innovative approaches to full-fill the fresh water need in most sustainable way. Single basin solar still is most utilized still owing to its simple construction, lower maintenance and lower cost of water generated through it [2]. However, the major drawback of this unit is limited receiver / condenser area (owing to the sloped cover exposed to the evaporation) which provide lower vapor exposure to the condenser and leads to lower water generation. In this regard, the increasing the condenser area could significantly increase the vapor accumulation on condenser, which in turn increases the fresh water generation. In this regard, hemispherical solar still (HSS) is getting significant attention in recent years owing to its large condensing / receiving surface area as compared to conventional single basin single

basin still [3]. The larger condenser area allows more vapour accumulation during the evaporation of water and increases the fresh water yield of the unit.

To optimize the suitable volume of feed-water in HSS basin, transportable type of HSS was designed by Ismail [4]. It was reported that the potable water produced is directly proportional to the water thickness inside the basin of HSS. With increasing thickness of water inside the basin, the potable water output was decreased and the same was observed in the case of daily efficiency. The water daily output from the proposed solar still with water thickness of 12, 14, and 18 mm were 4.7, 3.5, and 2.8 L/m^2 respectively. The basin material also plays a vital role in improving the HSS output and in this regard, Attia et al. [5] used different material such as wood, zinc, copper, and iron trays for fabricating the basin of HSS with an optimized water thickness of 10 mm. Results showed that the higher thermal conductivity of the copper tray augmented the freshwater produced by 31.25% than the conventional HSS using wood as the basin material. The cumulative freshwater produced from the HSS using the conventional tray with wood as basin material was only 4.8 L/m^2, which significantly increased to 5.5, 6.3, and 7.35 L/m^2 using iron, zinc, and copper trays respectively. Apart from the basin material, top cover cooling of hemispherical still using water is also an effective way to increase the yield and it was studied experimentally by Arunkumar et al. [6]. The driving force for enhanced condensation is the difference in water-cover temperature. On reducing the cover temperature, the driving force (partial pressure difference) was increased that simultaneously improved the condensation rate. Results showed that with an optimal cover cooling rate of 10 ml/min, the HSS thermal efficiency was augmented from 34% (without cooling- base HSS) to 42%. Similarly, there was an average improvement of 125% in freshwater production using the water cover cooling technique than the base HSS. Nano-suspended particle in feed-water also increased the freshwater yield owing to the improved thermal conductivity of the water with

nanoparticle suspension. Bellila et al. [7] studied the performance of HSS using Al_2O_3 nanoparticle suspended in feed-water. The nanoparticles were added to the feed-water in the concentration of 0.1, 0.2, and 0.3% by volume. Along with nanofluid, the effect on condensing surface cooling was studied to improve the rate of condensation. It was reported that under the climatic condition of Algeria, the traditional HSS could produce a maximum cumulative water yield of 3.28 L/m^2. On incorporating the proposed nanofluids (0.3 vol. %) in the basin along with cover cooling arrangement, the fresh water yield was enhanced by 120.1%. Attia et al. [8], used copper oxide nanofluid in the basin of HSS and used water cooling method to augment the potable water production. The cooling water flown over the cover were varied from 1.5 to 2.5 kg/hr, while the nanofluid concentration were varied from 0.1 to 0.3%. It was found that the addition of nanoparticle in the feed-water significantly improve the thermal conductivity and thereby improve the rate of evaporation. The potable water produced from the still was improved to about 49.3, 66.2 and 76.6 % using concentration of CuO nanoparticle as 0.1, 0.2 and 0.3% respectively as compared to bare HSS without any modification. Using water as working medium in the basin (without any suspension of nanoparticle) and sprinkler cover cooling arrangement over the head of HSS, the potable water production improved to about 27.3, 39 and 48 % for water flow rate of 1.5, 2 and 2.5 kg/hr respectively as compared to bare HSS. It was also concluded that the use of cover cooling and nanofluids appears to be economically viable as the cost of distilled water produced was significantly lower as compared to SS without any modification

Heat storage materials in form of sensible and latent storage are also being widely used to increase the thermal performance of the desalination unit. In sensible heat storage, the influence of sand grains as sensible heat-storing material in augmenting the clean water production of HSS was experimentally analyzed by Attia et al. [9]. Results reported that the cumulative yield and

daily efficiency of solar still were found as 7.27 L/m^2 and 59.1% respectively. The maximum improvement in the cumulative yield was found as 52.1%. For augmenting the performance of hemispherical solar still, Attia et al. [10] used internal reflectors and sand grains. Results reported that the combined effect of energy storage and focusing solar radiation augmented the clean water produced by 97.8% than the SS without modifications. It was also concluded that there was an improvement of about 49.1% in the cost per liter (CPL) of clean water produced. Experimental analysis and comparison of the productivity of tubular solar stills utilizing composite sensible energy storage materials in the tube were carried out by Elashmawy and Ahmed [11] and compared the same with traditional tubular solar still. The aluminium tubes were filled with sand material and copper wire and 12 tubes were placed in the absorber. In comparison to a solar still without energy storage material, the results revealed that the usage of energy storage improved the thermal efficiency by 20.06%. The CPL produced was lowered by 13% using energy storing material in a semicircular trough absorber. Elashmawy [12] used parabolic concentrating tracking to focus the incoming solar radiation to heat the absorber and store the heat energy using sensible material inside the basin to enhance fresh water production. Gravels were used as an energy storing material. It was reported that the sensible heat energy storing material with parabolic concentrator tracking produced a maximum cumulative yield of 4.51 L/m^2, whereas without tracking it was only 3.95 L/m^2 with energy storing material.

Latent heat storage in form of paraffin wax (as phase change material, PCM) is one of the most used methods to increase the water output of the solar still. Arunkumar and Kabeel [13] investigated the role of PCM on a yield of tubular SS with concentric pipe coupled collector. It was seen that usage of PCM enhanced water yield by 8% than the bare still without PCM. Dashtban and Tabrizi [14] examined cascade solar still coupled with paraffin wax of 18 kg mass and 2 cm

thick. It was found that PCM increased the water yield by 31% than the base still without PCM. Vigneswaran et al. [15] used concentric tubes filled with different kind of PCM with varying the phase change temperatures. The PCM-1 and PCM-2 with phase change temperature of 58.03–64.5 °C and 53.05–62 °C were used in tubes and compared with the single basin still without any PCM. The study observed that the water yield of still with PCM-1 and PCM-2 in combined was 8.6% greater than the still with only PCM-1. El-Sebaii et al. [16] numerically investigated the solar still with varying PCM mass and water depth and found that water yield in day-hours decreased while in night hours it increased and the overall water yield increased when higher mass of PCM was used. Thakur et al. [17] used PCM in cylindrical tube placed inside the basin of tubular still and result showed increased water yield of 42.4% than the base still.

Table 1 shows the existing literature on majorly HSS with various modifications for increasing the thermal performance. Nanoparticles in basin and cover cooling along with energy storage materials are the most widely adapted method for increasing productivity of solar still. From the literature review, it was also found that the energy storage materials predominantly PCM improves the performance of solar still. However, the majority of the researchers reported usage of PCM below the basin. In addition, the some researchers also used PCM encapsulation in the fabricated cylindrical tubes. It is important to understand that PCM placed beneath the basin could dissipate the majority of the stored energy to the basin enclosed walls and owing to the thickness of the basin material, the rate of heat transfer from the PCM to the basin water could be hindered. In addition, there is higher chance of heat losses to the surrounding ambient, although insulation is generally provided to the basin. In this regard, the effective placement of the PCM container in basin is a very critical factor. Majority of the reported work used metallic PCM encapsulation inside the basin (copper balls with PCM by Arunkumar et al. [18], Petroleum jelly-filled container

tubes by Ho et al. [19], fabricated aluminium tube with PCM by Elashmawy et al. [20]) which additionally increases the capital cost of the still and leads to higher freshwater cost per liter. In this regard, there is tremendous need to develop low-cost encapsulation material (which does not cause any additional cost on the still) with excellent thermal conductivity and without any leakage for avoiding any solar radiation blockage during the operation (PCM leakages in basin water can cause the solar radiation blockage).

Table. 1 Existing literature on HSS and its comparison with present work

Literature	Mechanism for enhancement	Modification	Water Yield (kg/m^2)	Inference
Arunkumar et al. [6]	Condensation	Water cover cooling method	4.2	Condensation was improved by flowing water as cooling medium.
Attia et al. [9]	Evaporation	Sand grains as energy storage	7.27	Different grain size of sand particles were experimentally analyzed. The optimal grain size for improved yield was found as 3 %.
Ismail [4]		Transportable type	5.7	Optimized water thickness was the only parameter analyzed.
Attia et al. [10]		Internal reflector and sand grains	9.4	Internal aluminium foil reflector and sand grains was added to the absorber for improved evaporation efficiency.
Attia et al. [12]	Evaporation and condensation	ZnO nanofluid and cover cooling	8.15	ZnO nanofluids used in the basin and using cover cooling at various mass flow rate of water over the cover the yield improved.
Bellila et al. [7]		Nanofluid (Al_2O_3-H_2O) with cover cooling	7.25	Metal oxide nanoparticle is mixed with salt water and furthermore condensation was improved using cover cooling method.
Attia et al. [8]		CuO nanofluids and cover cooling	6.8	Condensation is improved using inexpensive sprinklers and evaporation is improved using higher thermal conductivity CuO nanoparticle in fluid.
Present Study		4 PCM encapsulated can in hemispherical still	5.63	PCM increased the energy storage potential and improved the water yield significantly. 4 can arrangement increased water yield by 92.80%, whereas 3 can arrangement increased the yield by 67.12% than base case. Thus, higher mass increased more yield
		3 PCM encapsulated can in hemispherical still	4.88	

In addition, suitable placement of the PCM encapsulated container without leakage, preferably on the basin to effectively use the stored energy of PCM during charging / discharging is also required.

To the best of authors knowledge, discarded aluminium cans (a widely available waste-material) used for encapsulation of PCM with high-thermal conductivity and leak-proof structure has not been explored. In this prospective, present study effectively utilizes the theme of waste to energy by encapsulating paraffin wax into the waste aluminium cans (a very cheap and easily available encapsulating material with excellent leak-proof geometry and high thermal conductivity) placed into the basin of HSS for improving the water generation potential. In addition, the mass of PCM inside the encapsulated cans was firstly optimized and based on the results, only 80% of the cans were filled with PCM by considering the expansion and contraction of PCM during solidification and melting. After choosing the suitable mass of PCM and providing the clearance space in the cans for expansion and contraction, the PCM encapsulated cans were kept open from the top to capture the maximum falling solar radiation so as to perform faster charging / discharging cycle and improved thermal performance of HSS. In order to evaluate the performance of the solar still with aluminium cans and paraffin wax in terms of potable water production and energy efficiency, a comparative study of HSS with and without PCM was performed. In addition, cost analysis was also presented to give an overview of feasibility of the device. Water quality analysis was also done before and after the desalination to check its feasibility as drinking water.

2. Experimental setup and procedure

2.1. Experimental setup

To assess the role of phase change material (paraffin wax) and its cost effective encapsulation in increasing the water output of a novel shape solar distillation unit (i.e, HSS), the

present work was conducted in sunny days in month of November-December, 2021 on the roof of Center for Research and Development (CFRD), KPR Institute of Engineering and Technology, Coimbatore (10.55° N, 77.02° E), India. The HSS containing aluminium cans filled with paraffin wax is arranged in a triangular and square pattern and the entire scheme of the test-setup is shown in Fig. 1 and the photographic view of the test-setup with cans placed inside the basin is presented in Fig. 2. The top view of triangular pattern and square pattern is clearly visible in the image. Three different HSS: (i) conventional HSS without any PCM, (ii) HSS with 3 aluminium cans arranged in triangular pattern filled with paraffin wax, and (iii) HSS with 4 aluminium cans arranged in square pattern filled with paraffin wax were fabricated and experimental investigation. The basin area of the HSS was 0.1963 m^2 with an equivalent diameter of 0.25 m. The height of the hemispherical dome was fixed as 0.35 m from the bottom of the basin. The side wall height was fixed as 30 mm and the entire basin is fabricated using a mild steel sheet with thickness of 2 mm. The hemispherical dome was fabricated using 3 mm thick acrylic sheet. A flange is provided in both the basin side wall and acrylic dome in order to provide a tight fit and vapor leakage is avoided using a double-sided industrial tape. A high-density adhesive foam-insulation with 4 mm thickness was provided to avoid heat losses to the surrounding atmosphere. The distillate droplets formed on the inner acrylic cover glides due to the gravity and later, it reached the collecting channel mounted on the walls of hemispherical still and afterward, the hourly distilled collection was measured using a calibrated flask. Initially, the waste aluminium cylindrical cans with height of 15 cm and diameter of 5.3 cm were collected from local garbage collection center and thereafter it was thoroughly cleaned. It was ensured that the collected cans are cylindrical in shape and the dents were removed. The surface of the cans was polished and the paint was removed.

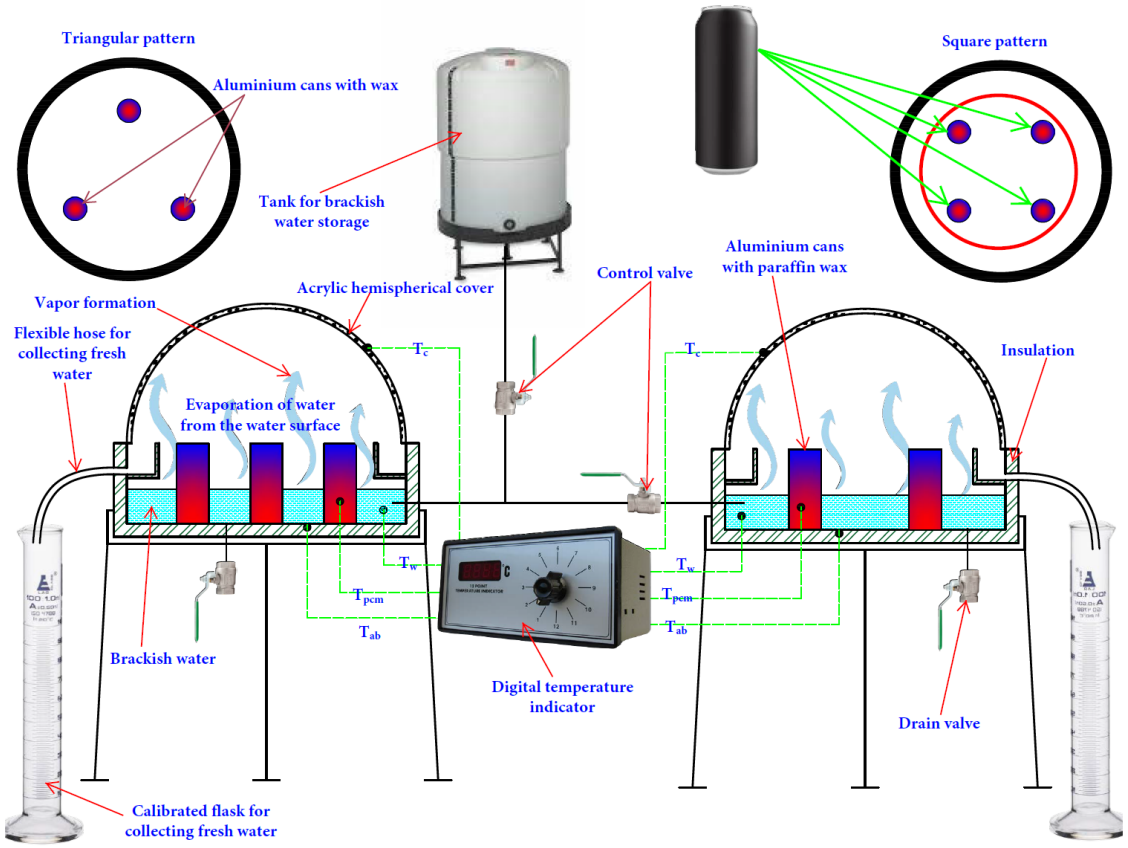

Fig. 1. Graphical representation of HSS with triangular and square pattern of PCM encapsulation

Fig. 2 Photograph of the experimental set-up with cans placed inside the basin

To increase the solar absorptivity of the PCM encapsulated cans, black paint was coated using spray and uniform coating was ensured. Fig. 3 shows the graphical procedure of preparation of aluminium cans with black powder coating. The filling of the PCM inside the cans and its positioning is presented in the following section.

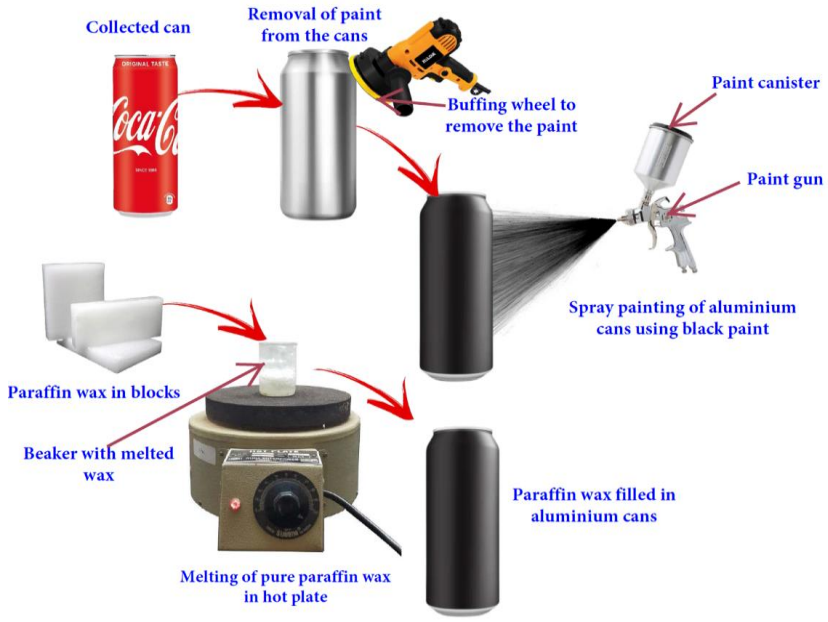

Fig. 3 Steps involved in preparation of paraffin wax encapsulation in cans

2.2. Paraffin encapsulation and its phase change characterization

For PCM encapsulation, it is very important to choose the right capsule geometry with low cost and good conductivity. Generally for macro-encapsulation of PCM, spherical, cylindrical, tube, cubical, spindle, drum etc shapes are widely used [21-22]. It is important to understand that encapsulation cost is an added burden on the system and it may significantly affect the overall effectiveness of the thermal storage unit in terms of economic. Höhlein et al. [23] recently reported

that metallic macro encapsulation cost was 17.91 euros including the fabrication, material and corrosion protection cost, however the PCM cost was just 0.22 euros. These studies reflected that the cost of encapsulation is a major factor in thermal energy storage and it should be reduced without compromising the thermo-physical behavior of the encapsulating material. In this regard, we have chosen the waste aluminium cans as can conductive encapsulating material for PCM. Initially, the commercial-grade paraffin wax was purchased from Nice Private Limited, Kerala, India and it was melted into liquid form using an electrical heater. Afterward, each aluminium cans were filled with the PCM and the thermo-physical properties of the PCM is tabulated in Table. 2. The PCM cans were filled only upto 80% of the can volume for providing the volume expansion/contraction during charging / discharging. It is also vital to note that the cans were kept open from the top after filling the PCM. For effective charging of the PCM, the direct solar radiation was allowed to fall on the PCM from the top of the open can space, which prompted faster rate of heat transfer owing to the direct exposed surface towards radiation. As the feed-water inside the basin was maintained at 3 cm depth, the filled cans with PCM was perfectly stable at its position owing to the weight of the PCM can. In addition, it was a cost effective approach also, as no sealant was required to seal the cans from top. The initially optimization of PCM volume was carried out to check the over flow of PCM from the can top and based on the outcomes, only 80% of the can was filled with the PCM.

Table. 2 Thermo physical properties of commercial grade paraffin wax

Property	Paraffin wax
Melting temperature (^{o}C)	58-60
Latent heat of fusion (J/kg)	187.28

Thermal conductivity (W/mK)	0.19
Density (kg/m^3)	914.2

After filling the cans with PCM, it was placed inside the basin of HSS. PCM cans were placed inside the basin radially and two different structure of cans were formed - in form of triangular pattern with 3 cans and in form of square pattern with 4 cans, as shown in Fig. 4 along with the PCM can opening space for filling the PCM.

Fig. 4 Pictorial view of PCM encapsulated cans placed in basin of HSS in triangular and square pattern with capsule opening provided for PCM filling

Two different shape of encapsulated cans were mainly used to optimize the mass of the PCM suitable for promoting higher water output. The phase change properties of the PCM such as latent heat, and phase change temperatures during freezing and melting were analyzed using differential scale calorimetry (DSC) (Q-20, TA Instrument). Thermo gravimetric analysis (TGA) was sued to check the decomposition and thermal stability of the PCM through SDT-Q600 (TA Instrument). The experimental test rig were equipped with 5 thermocouples in order to measure the temperature of still basin, PCM, water vapor, water, and acrylic cover. Similarly, the solar radiation falling on still was measured using the solar meter. The thermocouple used in the experiments is PT-100 type (RTD). The hourly-wind velocity and ambient temperature variations were measured using a vane-type anemometer. For comparing the thermal performance, the experimental conditions were considered to be similar. The experimental investigation were carried out for more than 15 times to ascertain its repeatability, and the HSS performance was nearly identical during the days of experimentation.

2.3. Uncertainty analysis

Based on the method by Holman [24], the uncertainty of the data is determined. U1, U2, U3, …. , Un is the independent variable on uncertainty and Ur will be the total uncertainty that occurred during the experiment. Mathematically it is expressed as,

$$U_Y = \left[\left(\frac{\partial Y}{\partial x_1} U_1 \right)^2 + \left(\frac{\partial Y}{\partial x_2} U_2 \right)^2 + \left(\frac{\partial Y}{\partial x_3} U_3 \right)^2 + ... + \left(\frac{\partial Y}{\partial x_n} U_n \right)^2 \right]^{0.5} \quad (1)$$

The uncertainty occurred during the experiments on distilled water production is given as,

$$U_m = \left[\left(\frac{\partial m}{\partial n_1} U_n \right)^2 \right]^{0.5} \quad (2)$$

Similarly, the uncertainty occurred in calculating the thermal efficiency is expressed as,

$$U_\eta = \left[\left(\frac{\partial \eta}{\partial m} U_m \right)^2 + \left(\frac{\partial \eta}{\partial I(t)} U_{I(t)} \right)^2 \right]^{0.5} \quad (3)$$

Range, accuracy and uncertainty of the different measuring components is tabulated in Table 3.

Table. 3 Accuracy, range, uncertainty of measuring instruments

Instrument	Range	Accuracy	Uncertainty
RTD sensors	-250 to 1000^{o}C	± 0.3°C	± 1.33
Solar power meter	0-3500 W/m^2	± 10 W/m^2	± 4.24
Anemometer	0-45 m/s	± 0.05 m/s	± 3.45
Distillate flask	0-1000 ml	± 10 ml	± 5.67

2.4. Daily distillation thermal efficiency

The daily distillation thermal efficiency is defined as the ratio of cumulative fresh-water produced during the entire day and latent heat of vaporization to the amount of solar radiation as heat input. It is mathematically given as [25],

$$\eta_{thermal} = \frac{\Sigma m_e \times L_{fg}}{\Sigma I(t) \times A_{HSS}} \times 100 \quad (4)$$

3. Water quality analysis

The quality of water produced from the distillation unit is also a critical parameter apart from the amount of potable water produced. For the present study, the ground water from Industrial

area (Arasur, Coimbatore, India) was collected and used as the feed water in the present study. Distilled water and un-treated water quality is tabulated in Table. 4. The outcomes shows that the water after desalination is within the allowable tolerance limit prescribed by IS 10500-2012 Indian standards [26].

Table. 4 Water quality assessment

Parameter tested	Before desalination	After desalination	Drinking tolerance
pH	7.5	6.5	6.5-8.5
Electrical conductivity (μS/cm)	1100	25	-
TDS (ppm)	870	28	500
Total hardness (ppm)	645	23	200
Calcium (ppm)	290	18	75
Alkalinity (ppm)	400	15	200

4. Result and discussions

4.1. Mechanism of heat transfer during charging and discharging of PCM

Fig. 5 shows the mechanism of heat transfer from the PCM encapsulation during charging and discharging cycle with open space on top of the encapsulation for increasing the direct absorption of falling solar radiation. As depicted in the figure, only 20% (3 cm) of the encapsulation is immersed in the feed-water and remaining 80% (12 cm) of the encapsulation is exposed to direct falling radiation. During charging process, the solar radiation transmitted through

the transparent acrylic cover direct falls on the radially kept cans which is open from top and the solar energy starts melting the PCM initially from the upper surface.

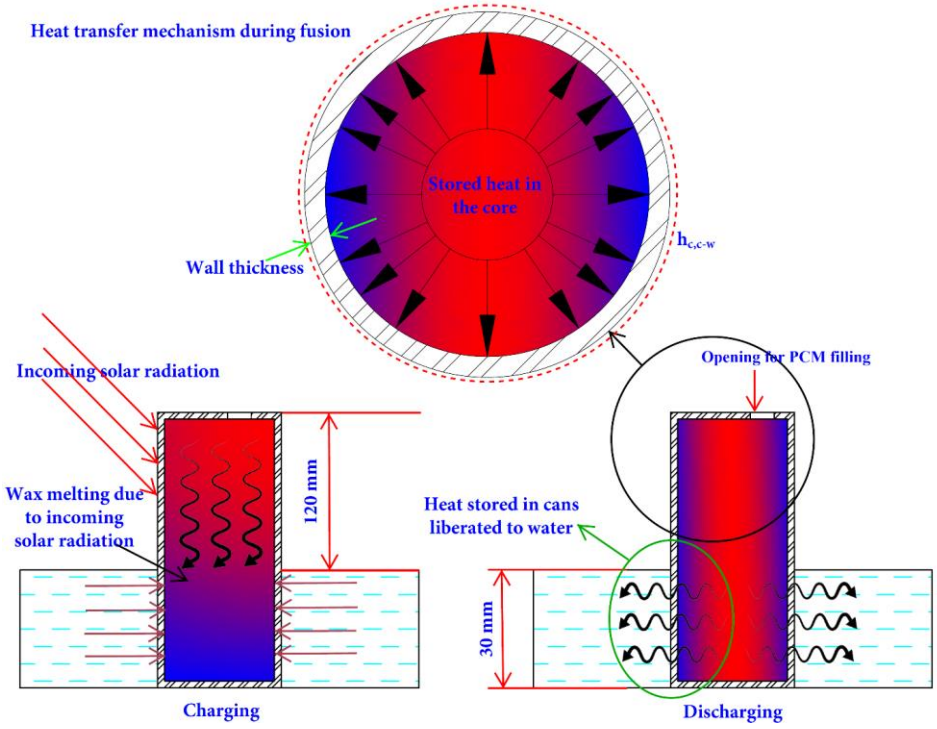

Fig. 5 Heat transfer during charging/discharging of PCM from encapsulation

As the cans are kept open from top, the PCM melting first takes place at the upper exposed surface and later, the heat propagated from top to the bottom of the cans. In addition, the stored energy on the feed-water inside the basin was also transferred to the encapsulated PCM from the bottom side, which is immersed in the water. Thus, there will be synergetic heating of PCM from the open top exposed surface directly via solar radiation and from the bottom via the feed-water. The simultaneous heating of encapsulated PCM increases the temperature to achieve its faster melting.

During the discharging process, the energy stored in the inner core of PCM will release the stored heat to the water for attaining an optimal water temperature, even during off-peak solar radiation hours and improved heat transfer.

4.2. Phase change analysis of PCM

The major phase change behavior was examined using DSC. The DSC curve of paraffin wax in the exothermic and endothermic processes is plotted in Fig. 6. It is seen that the latent heat during the heating is found as 187.28 J/kg, whereas, during the freezing, it is found as 163.57 J/kg. It is observed that a single endothermic and exothermic peak occurred at 52.01°C and 58.53°C respectively. The peak clearly depicts the phase transformation from solid to liquid and liquid to solid phase for endothermic and exothermic processes respectively. From TGA analysis, the complete decomposition of PCM was at 347°C and the initial decomposition was at 225°C.

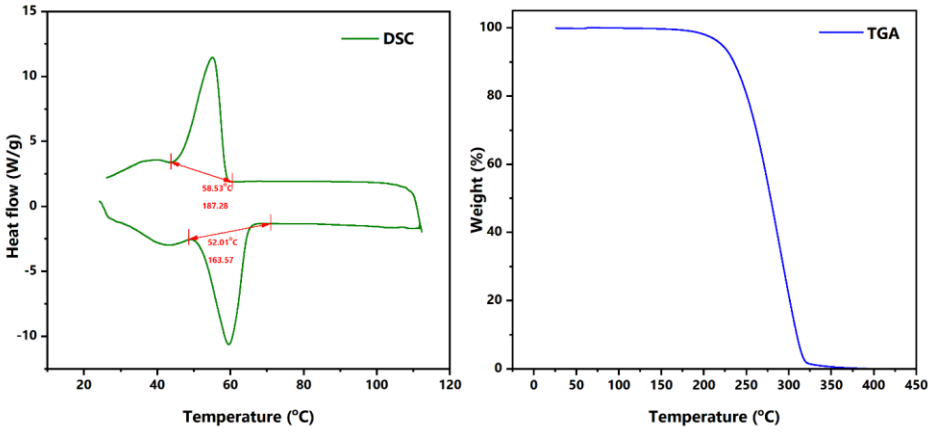

Fig. 6 DSC and TGA curve of PCM

4.3. Thermal performance and water yield analysis of HSS

The thermal performance of the HSS such as water yield, and thermal efficiency are determined in a quantitative way using the measured parameters such as ambient, cover, water, and absorber temperature, wind velocity, and solar radiation. The experiments were conducted in three different modes namely, (i) HSS, (ii) HSS with 3 aluminium cans (triangular pattern), and (iii) HSS with 4 aluminium cans (square pattern) to evaluate the most suitable mass of encapsulated PCM. The variations on the temperature of the cover, ambient, absorber, and water wind velocity, and solar radiation of HSS without energy storage is plotted in Fig. 7. Similarly, the variations on HSS using 3 aluminium cans (triangular pattern) and 4 aluminium cans (square pattern) are plotted in Fig. 8 (a) and (b). The important parameter that drives the solar still is the solar radiation. For the comparison, measured parameters and the daily solar radiation are taken for the same day.

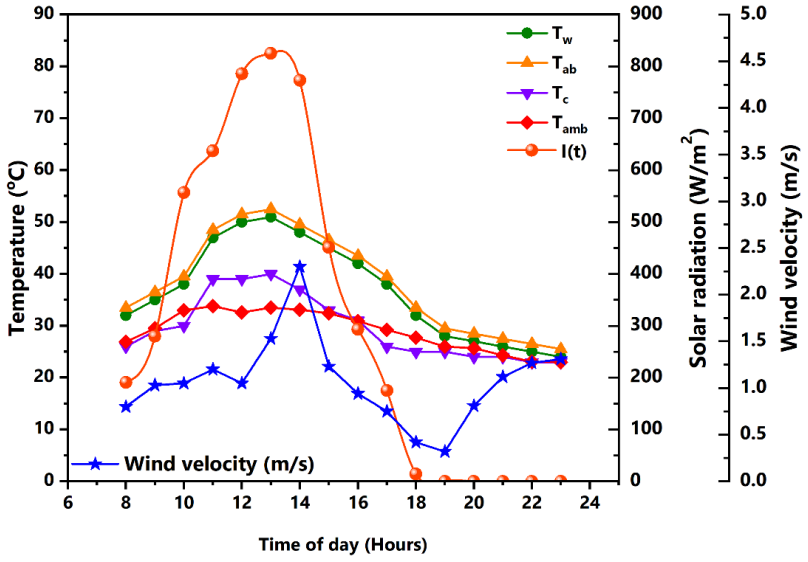

Fig. 7 Variations on the temperature of water, absorber, cover and ambient, wind velocity, and solar radiation of conventional HSS

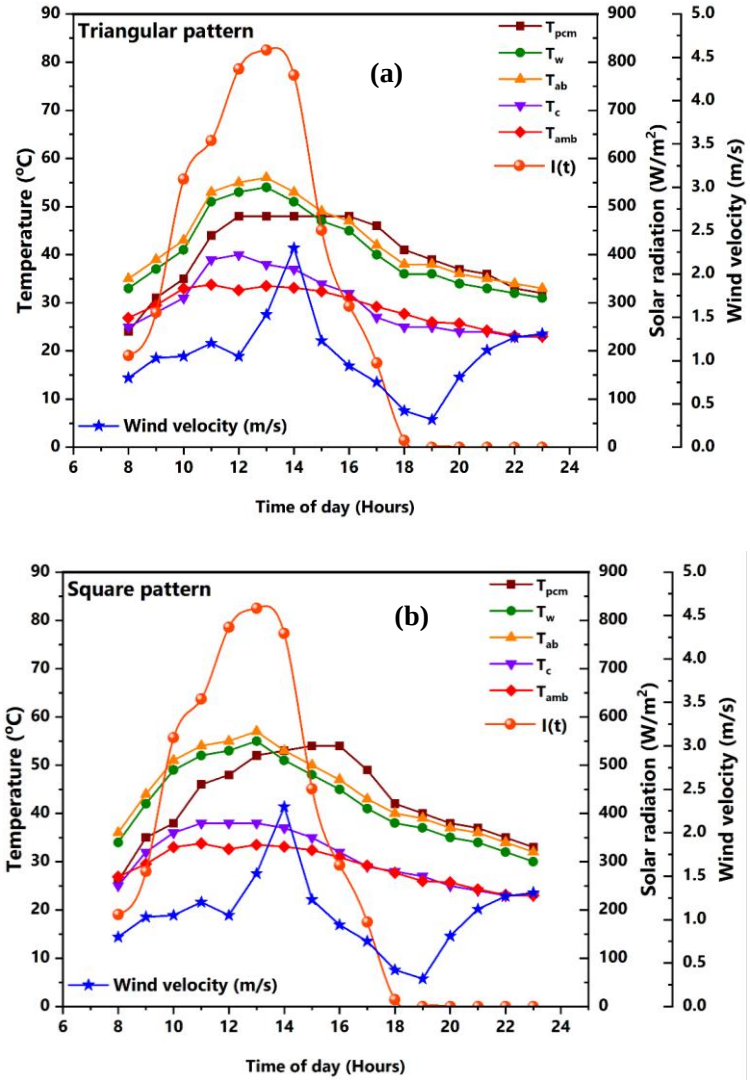

Fig. 8 Variations on the temperature of PCM, water, absorber, cover and ambient, wind velocity, and solar radiation of HSS with (a) 3 aluminium cans and (b) 4 aluminium cans with PCM

The solar radiation falling on the horizontal surface varied from 5 to 910 W/m^2 with an average ambient temperature of 31.5°C. It is seen that peak recorded water, cover, absorber temperature of HSS without PCM were 50, 39, and 51°C respectively. In contrast, the HSS with PCM encapsulated in triangular pattern cans recorded a peak temperature of 53, 40, and 55°C for water, cover, and absorber respectively (Fig. 8 a). The increase in water temperature is due to the effect of heat stored in PCM, which simultaneously rejects its heat at the lower temperature. Also, the temperature of the PCM is lower in the aluminium can at 16:00 hrs and during the off-shine hours, the water gained the heat from the cans filled with PCM for increased temperature as compared to the HSS without PCM. The PCM filled in the cans reaches its melting temperature at a short time interval as 80% of the cans was exposed to incoming solar radiation and vapor available inside the hemispherical enclosure. It is also seen that using encapsulated PCM, the water temperature enhanced by 12% as compared to HSS without PCM. Similarly, the effect of arranging the aluminium cans in triangular and square patterns is studied on thermal performance. Since the PCM was placed in the aluminium cans, the heat transfer was superior owing to the higher conductivity of aluminium which allows faster transfer of heat.

The variations on water, absorber, cover, and PCM temperature of HSS using triangular and square patterns is presented in Fig. 8 (a) and (b). It is seen that the charge of heat for the paraffin wax is shorter as the cumulative mass of paraffin wax is 1.2 kg in the cans for the triangular pattern, while the discharge is also shorter. For a square pattern, the amount of paraffin wax filled in the cans is 1.6 kg which provided a longer period for discharge for extended time during the night time operations. The temperature of PCM for both triangular and square patterns is more than the temperature of the water during night hours. It was observed that the temperature of the water using a triangular encapsulation PCM can pattern is lower than the square PCM

encapsulation pattern. It is obvious that the higher mass of PCM in the square pattern exhibited higher energy storage and later, it was discharged to increase the water temperature. Also, the increased exposure of area provided equilibrium of heat to be transferred from PCM cans and the water surroundings. The even distribution of heat from the aluminium cans with liquid PCM is attributed to an enhanced temperature of the water. With higher water temperature, the rate of water vapor accumulated in the hemispherical cover increases which simultaneously enhanced the cover temperature. It is well known that the temperature difference between the water and transparent cover plays an important role in increasing the water yield and it should be higher for achieving the optimal results. The HSS using three PCM encapsulated cans in triangular pattern exhibited an average difference in temperature (water-cover) of about 10.93°C, it further increased to 11.62°C with the SS with four PCM encapsulated cans in square pattern. However, the average temperature difference of water-cover was only 7.12°C for bare HSS without PCM. Therefore, average increase in temperature difference between water and cover were 53.51% and 63.20% respectively with PCM cans in a triangular pattern and square pattern as compared to HSS without PCM. In addition, the peak temperature difference of water-cover during the peak solar radiation period were 11°C, 16°C, and 17°C for bare HSS, HSS with 3 PCM encapsulated cans, and HSS with 4 PCM encapsulated cans respectively.

The transient variations in temperature of PCM during charging and discharging of heat from PCM encapsulated can to water is plotted in Fig. 9 (a) and (b). It is seen that the temperature of PCM is higher in PCM encapsulated can arranged in a square pattern (4 cans) as compared to PCM encapsulated can in triangular pattern (3 can). The synergetic heating from feed water and solar radiation causes the maximum temperature of PCM to 54°C in square can arrangement whereas in triangular can arrangement, PCM reached a maximum temperature of only 46°C.

During the discharge of heat from the PCM encapsulated can, the temperature of PCM steadily decreases for attaining higher water temperature. There is an increase in about 2°C - 2.5°C in the PCM temperature using square PCM can pattern as compared to triangular PCM can pattern.

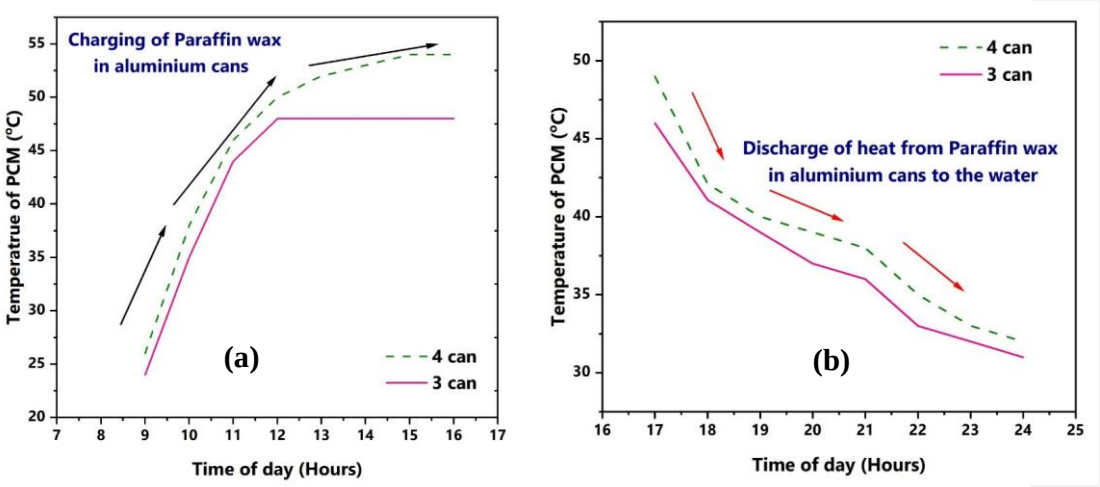

Fig. 9 Variations on PCM temperature with respect to time (a) charging and (b) discharging

The main focus of present work is to explore the role of PCM optimized mass filled in aluminium can on increasing the water yield of HSS and it is presented in this section. The important factors which needs to be measured is the hourly and cumulative water yield obtained during the experimental hours to assess the overall performance of HSS. Fig. 10 and 11 show the variations on hourly water produced and cumulative full day water produced by HSS with and without paraffin wax in aluminium cans during the experiments. The hourly potable water produced by HSS followed a similar trend like solar radiation for all the cases. Moreover, it is observed that the yield of water from the HSS with PCM filled in cans arranged on a square pattern

was higher followed by the water produced using triangular pattern and HSS without any energy storing material.

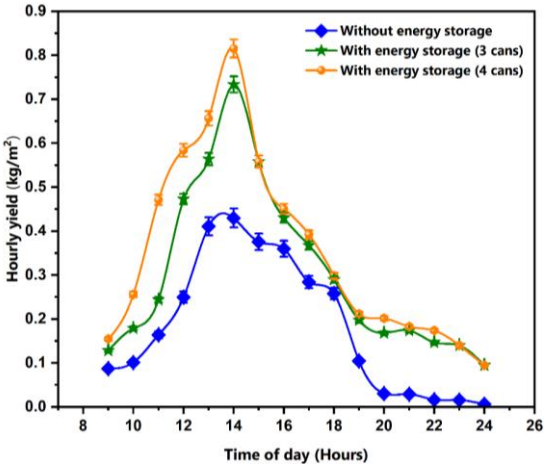

Fig. 10 Hourly variations on potable water from three different configurations

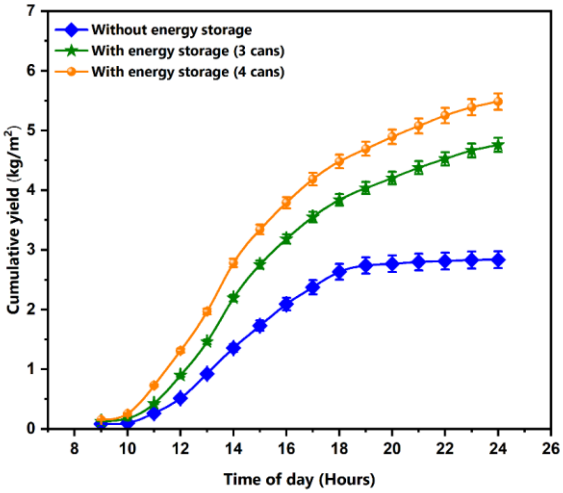

Fig. 11 Hourly variations on cumulative yield from three different configurations

The peak recorded water production from HSS, HSS with 3 cans (triangular pattern) and HSS with 4 cans (square pattern) were 0.42 kg/m^2, 0.73 kg/m^2 and 0.81 kg/m^2 at 14:00 Hrs respectively. It is obvious that the higher PCM mass in square pattern of encapsulated can allows to store more energy and leads to achieve higher hourly yield. Cumulative water yield produced by conventional HSS was 2.92 kg/m^2 which was significantly increased to 67.12% and 92.80% with 3 and 4 PCM can respectively. The improved yield of potable water from the HSS with PCM is mainly due to higher water temperature using cans filled with PCM with excellent energy storage potential that causes faster evaporation and produced higher yield.

Table. 5 compares the daily yield, efficiency, improvement in yield of modified solar still with PCM cans arranged in triangular and square pattern and without PCM cans in the basin. The daily distillation thermal efficiency of HSS, HSS with 3 cans, and HSS with 4 cans filled with paraffin wax are calculated as 30.9, 53.35, and 61.55% respectively. It was found that the distillation thermal efficiency directly relay on the PCM mass, as higher mass (4 cans with paraffin wax) generated more water, and the thermal efficiency (Equation 1) shows that it is directly related to the water yield. Thus, PCM with 4 can owing to more mass exhibited higher thermal efficiency. It was also seen that the for the same daily total solar radiation of 5741 W/m^2, the cumulative yield improved significantly for triangular and square PCM can arrangement. Similarly, the average water temperature throughout the day for HSS without PCM cans and with PCM cans arranged in triangular and square pattern was found to be 36.75°C, 40.62°C and 42.25°C respectively, whereas there was no significant variations on the average cover temperature during the experimentation. It is also clearly observed from the outcomes that the use of discarded aluminium cans provide a potential interest towards storage of heat in the form of latent heat.

Table. 5 Comparison of daily yield, efficiency, improvement in yield of HSS with and without PCM

Type	Daily yield (L/m^2)	Daily distillation thermal efficiency (%)	Yield improvement (%)	Daily solar radiation (W/m^2)	Average absorber temperature (°C)	Average water temperature (°C)	Average cover temperature (°C)	Average difference in temperature between water and cover (°C)
HSS	2.92	31.90	-		38.25	36.75	29.62	7.12
HSS with 3 PCM cans	4.88	53.35	67.12	5741	42.62	40.62	29.68	10.93
HSS with 4 PCM cans	5.63	61.55	92.80		44.25	42.25	30.62	11.62

5. Economic analysis

The cost involved in the fabrication of HSS is tabulated in Table. 6. Similarly, the cost per liter of water produced from SS depends on cost factors such as cost on fabrication (fixed), annual cost (fixed), maintenance cost, salvage value, and annual cost. Also, the annual yield of potable water produced is another factor to determine the cost per liter of water. The following assumptions were made to determine the capital recovery factor and sinking fund factor.

i = 10 %, and n = 10 years

where, i- is the rate of interest (%) and n- is the life span of SS.

For the calculation of annual yield, it is considered that 292 days of clear sky conditions exist. The correlation for determining the FAC, CRF, SFF, salvage, annual salvage, AMC, TAC, and CPL are tabulated in Table. 7. Table. 8 shows calculated values of FAC, ASV, AMC, TAC, and CPL are tabulated. It can be seen that the CPL of water from HSS, HSS with energy storage arranged in a triangular pattern, and HSS with energy storage arranged in the square pattern are 0.0186, 0.0128, and 0.0111 $/L respectively.

Table. 6 Cost of fabricating HSS

Component	Cost ($)
Acrylic cover	35
Piping, control valve, fittings and hose connections	25
Stand	10
Feed water storage tank	5
Insulation foam	5

Fabrication cost of basin	20
Black paint	2
Total cost on HSS ($)	102
Paraffin wax	16
Aluminium cans	0.1 per Al-can
Total cost on HSS with energy storage (triangular pattern)	118.3
Total cost on HSS with energy storage (square pattern)	118.4

Table. 7 Correlations for economic analysis [27]

Cost component	Correlation
CRF	$\frac{i(1+i)^n}{(1+i)^n-1}$
FAC	$F \times CRF$
SFF	$\frac{i}{(1+i)^n-1}$
S	$0.2 \times F$
ASV	$S \times SFF$
AMC	$0.15 \times FAC$
TAC	$FAC + ASV - AMC$
CPL $\frac{TAC}{M}$	(M = Average yield x 292 days)

Table. 8 Economic analysis on CPL of different configurations of solar still

Cost component	HSS	HSS with energy storage (aluminium cans arranged in triangular pattern)	HSS with energy storage (aluminium cans arranged in square pattern)
Total cost on fabrication ($)	102	118.3	118.4
Fixed annual cost (FAC) ($)	16.60	19.25	19.26
Annual salvage value (ASV) ($)	1.28	1.48	1.48
Maintenance cost (AMC) ($)	2.49	2.88	2.89
Annual cost (TAC) ($)	15.39	17.84	17.86
Annual yield (L/m^2)	826.36	1387	1600.16
CPL ($/L)	**0.0186**	**0.0128**	**0.0111**

6. Enviro-economic analysis

Considering CO_2 generated owing to coal power plants operations as 1.58 kg/kWh, the mitigation of CO_2 and carbon credit earned via usage of HSS and modified HSS were studied by following relations [28-33].

CO_2 emission during entire life-span of HSS (kg) = $E_{in} \times 1.58$ (5)

CO_2 mitigation during the entire life-span of HSS (kg) = $E_{out} \times n \times 1.58$ (6)

n is life span of HSS which is 10 years.

The yearly energy output (E_{out}): $$E_{out} = \frac{m_e \times L_{fg}}{3600} \quad (7)$$

The net mitigation of CO_2 (T) during HSS lifespan is determined by:

$$M_{CO_2} = \frac{1.58 \times \left[E_{out} \times n - E_{in}\right]}{1000} \quad (8)$$

The carbon credit earned (CC) is determined as follow:

$$CC = C_{CO_2} \times M_{CO_2} \quad (9)$$

where the C_{CO2} (carbon international price) is taken as 14.5 \$/T,$_{CO2}$ for the calculation.

The results of the enviro-economic analysis of HSS is presented in Table 9 and 10. Table 9 shows the total embodied energy (E_{in}) of the components of the HSS and types of materials used in this investigation. E_{in} of HSS, HSS with 3 PCM can and HSS with 4 PCM can were 173.8 kWh, 441.8 kWh and 531.1 kWh, respectively. It was observed that the net CO_2 mitigations were 8.19 tons, 13.44 tons and 15.4 tons for bare HSS, HSS with 3 PCM can and HSS with 4 PCM can, respectively. It is clearly seen that CO_2 mitigation higher with the PCM. As the embodied energy of paraffin wax is 198.3 kWh/kg [31], the net CO_2 mitigation increased. Therefore, in view of the environmental effects, these systems an excellent way to reduce the carbon footprint of producing drinking water. The maximum carbon credits earned were estimated to be 118.7 \$, 194.8 \$ and 223.3 \$ for the bare HSS, HSS with 3 PCM can and HSS with 4 PCM can, respectively as shown in Table 10.

Table. 9 The embodied energy of HSS components

HSS components	Materials	Embodied energy (E_{in})		
		HSS (kWh)	HSS - 3 PCM Can (kWh)	HSS - 4 PCM Can (kWh)
HSS basin wall + absorber	Mild Steel	83.33	83.33	83.33
Acrylic cover	Acrylic	70.75	70.75	70.75
Insulation	Foam	3	3	3
Basin coating	Black paint	8.5	8.5	8.5
PCM Cans	Aluminium	-	29.97	39.96
Paraffin wax (PCM)	Paraffin	-	237.96	317.28
Control valve and sealing	Silicon rubber	6.9	6.9	6.9
Nut and Bolt	Iron	1.4	1.4	1.4
Total embodied energy (E_{in})		**173.8**	**441.8**	**531.1**

Table. 10 HSS enviro-economic analysis

SS type	HSS	HSS - 3 PCM Can	HSS - 4 PCM Can
Annual water yield (kg)	853	1425	1644
E_{in} (kWh)	173.8	441.8	531.1
E_{out} (kWh)	536	895	1032
CO_2 emissions (kg)	275	699	840
Net CO_2 mitigation (tons)	8.19	13.44	15.4
CC (US $)	118.7	194.8	223.3

7. Conclusions

In the present work, augmentation achieved in the fresh water yield achieved from the hemispherical solar stills with PCM is compared with the fresh water yield achieved from the conventional hemispherical still. Hemispherical solar stills were integrated with PCM encapsulated in aluminium can (which was kept open from top) in two different pattern namely triangular pattern of can with 3 PCM can and square pattern of can with 4 PCM can and experimental analysis of the effect on PCM mass encapsulated in the can on the thermal performance was carried out under the geographical conditions of Coimbatore, India. As the aluminium can were widely available as the waste material and it possesses excellent thermal conductivity, the PCM was encapsulated in it for storing the storing the energy. During lower solar intensity period and after the sun-shine period, the can encapsulated PCM acts as a heat reservoir for the feed-water available in the HSS basin. This facilitated maintenance of the higher temperature difference between water-cover. HSS with waste aluminium cans contained PCM boosted the temperature difference between water and cover and also assisted in keeping the HSS basin water temperature at a higher level for a lengthier period during the night hours. The recommendation made from the finding of the study is that usage of waste aluminium can with higher mass of PCM (filled in 4 cans with square pattern of the can), as low cost encapsulating material for latent heat storage in HSS results in an considerable improvement of the water yield during sunshine and off-sunshine hours. Apart from the aforementioned recommendation, the experimental study have provided the following conclusions:

- The maximum recorded temperature of the water, cover, absorber from HSS without any energy storing material were 50, 39, and 51°C respectively. In contrast, the HSS with PCM

encapsulated can arranged in a triangular pattern recorded a peak temperature of 53, 40, and 55°C from the water, cover, and absorber respectively.

- The average temperature difference between water and cover for the SS without PCM was found to be 7.12°C, whereas usage of PCM encapsulated in the aluminium can with triangular pattern (3 cans) and square pattern (4 cans) increase the temperature difference to 10.93°C, and 11.62°C, respectively. The excellent energy storage potential of the PCM leads to significant increase in the temperature difference.
- The peak-hourly freshwater produced from HSS, HSS with 3 cans (triangular pattern), and HSS with 4 cans (square pattern) were 0.42, 0.73 ad 0.81 kg/m^2 respectively. Cumulative full-day water produced by bare HSS was 2.92 kg/m^2 and it was significantly increased to 67.12% and 92.80% with 3 PCM encapsulated can and 4 PCM encapsulated can arrangement, respectively.
- The daily distillation thermal efficiency of HSS, HSS with 3 PCM encapsulated can and 4 PCM encapsulated can arrangement were 30.9%, 53.35%, and 61.55% respectively.
- The CPL of water from HSS, HSS with energy storage arranged in a triangular pattern, and HSS with energy storage arranged in square pattern are 0.0186, 0.0128, and 0.0111 $/L respectively.
- The modified HSS with 3 PCM cans and 4 PCM cans reduced the lifetime CO_2 emissions by 13.44 and 15.4 tons during their lifespan of 10 years, and with large area positioning, the HSS would considerably decrease the carbon footprint of the water purification industry.

8. Future recommendation

It has been found from the present study that PCM encapsulation in aluminium discarded can give excellent encapsulation stability and it was a cost effective method for encapsulating PCM. With higher mass of PCM in square pattern of the aluminium cans (4 cans), water yield was significantly higher than the triangular pattern aluminium with 3 can. Moreover, it is suggest to explore the effect of same PCM mass filed in can in form of triangular and square pattern to optimize the best structure of encapsulated can in form of triangular or square. It is also suggested to explore the role of nano-coated conductive materials such as activated carbon [34], reduced graphene oxide [35] or the composite nanoparticle on the cans for increasing the solar absorptivity and thermal performance of the energy storage materials.

Nomenclature

A_{Hss}	:	Area of still cover (m^2)
E_{in}	:	Embodiment input energy (kWh)
E_{out}	:	Energy output (kWh)
I_t	:	Solar radiation (W/m^2)
L_{fg}	:	Latent heat of evaporation (J/kg)
m_e	:	Water yield (kg)

Greek symbol

$\eta_{thermal}$	:	Daily distillation thermal efficiency

Abbreviation

CC	:	Carbon credit earned
CPL	:	Cost per liter of water
HSS	:	Hemispherical solar still
PCM	:	Phase change materials
TDS	:	Total dissolved solid

CRediT authorship contribution statement

Thamarai Kannan B: Formal analysis, Writing – review & editing. **B. Madhu:** Formal analysis, Writing – review & editing. **AE Kabeel:** Methodology, Validation, Writing – review & editing. **Amrit Kumar Thakur:** Conceptualization, Methodology, Validation, Formal analysis, Data curation, Investigation, Writing - original draft, Writing – review & editing. **R. Velraj:** Conceptualization, Methodology, Writing - review & editing, Supervision. **I. Lynch:** Methodology, Data curation, Writing - review & editing, Validation **R. Saidur:** Data curation, Methodology**,** Writing - review & editing. **Ravishankar Sathyamurthy:** Conceptualization, Investigation, Resources, Data curation, Writing - review & editing, Supervision, Project administration.

Declaration of competing interest

The authors declare that they have no known competing financial interests or personal relationships that could have appeared to influence the work reported in this paper

Acknowledgement: R. Saidur would like to acknowledge the support from the Sunway University under the Research Cluster project # STR-RCGS-MATSCI[S]-001-2021.

References

1. Sathyamurthy, R., El-Agouz, S.A., Nagarajan, P.K., Subramani, J., Arunkumar, T., Mageshbabu, D., Madhu, B., Bharathwaaj, R. and Prakash, N., 2017. A review of integrating solar collectors to solar still. *Renewable and Sustainable Energy Reviews*, *77*, pp.1069-1097.
2. Thakur, A.K., Sathyamurthy, R., Saidur, R., Velraj, R., Lynch, I. and Aslfattahi, N., 2022. Exploring the potential of MXene-based advanced solar-absorber in improving the

performance and efficiency of a solar-desalination unit for brackish water purification. Desalination, 526, p.115521.

3. Attia, M.E.H., Kabeel, A.E., Abdelgaied, M., El-Maghlany, W.M. and Bellila, A., 2021. Comparative study of hemispherical solar distillers iron-fins. Journal of Cleaner Production, 292, p.126071.
4. Ismail, B.I., 2009. Design and performance of a transportable hemispherical solar still. Renewable Energy, 34(1), pp.145-150.
5. Attia, M.E.H., Kabeel, A.E., Abdelgaied, M., Essa, F.A. and Omara, Z.M., 2021. Enhancement of hemispherical solar still productivity using iron, zinc and copper trays. Solar Energy, 216, pp.295-302.
6. Arunkumar, T., Jayaprakash, R., Denkenberger, D., Ahsan, A., Okundamiya, M.S., Tanaka, H. and Aybar, H.Ş., 2012. An experimental study on a hemispherical solar still. Desalination, 286, pp.342-348.
7. Bellila, A., Attia, M.E.H., Kabeel, A.E., Abdelgaied, M., Harby, K. and Soli, J., 2021. Productivity enhancement of hemispherical solar still using Al2O3-water-based nanofluid and cooling the glass cover. Applied Nanoscience, 11(4), pp.1127-1139.
8. Attia, M.E.H., Kabeel, A.E., Abdelgaied, M. and Abdelaziz, G.B., 2021. A comparative study of hemispherical solar stills with various modifications to obtain modified and inexpensive still models. Environmental Science and Pollution Research, 28(39), pp.55667-55677.
9. Attia, M.E.H., Kabeel, A.E. and Abdelgaied, M., 2021. Optimal concentration of El Oued sand grains as energy storage materials for enhancement of hemispherical distillers performance. Journal of Energy Storage, 36, p.102415.

10. Attia, M.E.H., Kabeel, A.E., Abdelgaied, M. and Shmouty, A.R., 2022. Enhancing the hemispherical solar distiller performance using internal reflectors and El Oued sand grains as energy storage mediums. Environmental Science and Pollution Research, 29(15), pp.21451-21464.
11. Elashmawy, M. and Ahmed, M.M., 2021. Enhancing tubular solar still productivity using composite aluminum/copper/sand sensible energy storage tubes. Solar Energy Materials and Solar Cells, 221, p.110882.
12. Elashmawy, M., 2020. Improving the performance of a parabolic concentrator solar tracking-tubular solar still (PCST-TSS) using gravel as a sensible heat storage material. Desalination, 473, p.114182.
13. Arunkumar, T. and Kabeel, A.E., 2017. Effect of phase change material on concentric circular tubular solar still-Integration meets enhancement. Desalination, 414, pp.46-50.
14. Dashtban, M. and Tabrizi, F.F., 2011. Thermal analysis of a weir-type cascade solar still integrated with PCM storage. Desalination, 279(1-3), pp.415-422.
15. Vigneswaran, V.S., Kumaresan, G., Dinakar, B.V., Kamal, K.K. and Velraj, R., 2019. Augmenting the productivity of solar still using multiple PCMs as heat energy storage. Journal of Energy Storage, 26, p.101019.
16. El-Sebaii, A.A., Al-Ghamdi, A.A., Al-Hazmi, F.S. and Faidah, A.S., 2009. Thermal performance of a single basin solar still with PCM as a storage medium. Applied Energy, 86(7-8), pp.1187-1195.
17. Thakur, A.K., Sathyamurthy, R. and Velraj, R., 2022. Development of candle soot dispersed phase change material for improving water generation potential of tubular solar distillation unit. Solar Energy Materials and Solar Cells, 241, p.111748.

18. Arunkumar, T., Denkenberger, D., Velraj, R., Sathyamurthy, R., Tanaka, H. and Vinothkumar, K.J.E.C., 2015. Experimental study on a parabolic concentrator assisted solar desalting system. Energy Conversion and Management, 105, pp.665-674.
19. Ho, Z.Y., Bahar, R. and Koo, C.H., 2022. Passive solar stills coupled with Fresnel lens and phase change material for sustainable solar desalination in the tropics. Journal of Cleaner Production, 334, p.130279.
20. Elashmawy, M., Alhadri, M. and Ahmed, M.M., 2021. Enhancing tubular solar still performance using novel PCM-tubes. Desalination, 500, p.114880.
21. Tian, Y., Liu, X., Zheng, H., Xu, Q., Zhu, Z., Luo, Q., Song, C., Gao, K., Yao, H., Dang, C. and Xuan, Y., 2022. Artificial mitochondrion for fast latent heat storage: Experimental study and lattice Boltzmann simulation. Energy, p.123296.
22. Wei, J., Kawaguchi, Y., Hirano, S. and Takeuchi, H., 2005. Study on a PCM heat storage system for rapid heat supply. Applied thermal engineering, 25(17-18), pp.2903-2920.
23. Höhlein, S., König-Haagen, A. and Brüggemann, D., 2018. Macro-encapsulation of inorganic phase-change materials (PCM) in metal capsules. Materials, 11(9), p.1752.
24. Holman, J. P. (2012). Experimental methods for engineers. (Eighth ed.), McGraw-Hill Companies, New York.
25. Thakur, A.K., Sathyamurthy, R., Velraj, R., Saidur, R. and Hwang, J.Y., 2021. Augmented performance of solar desalination unit by utilization of nano-silicon coated glass cover for promoting drop-wise condensation. Desalination, 515, p.115191.
26. Thakur, A.K., Sathyamurthy, R., Velraj, R. and Lynch, I., 2022. Development of a novel cellulose foam augmented with candle-soot derived carbon nanoparticles for solar-powered desalination of brackish water. Environmental Science: Nano. 9, 1247-1270

27. Kabeel, A.E., Sathyamurthy, R., Sharshir, S.W., Muthumanokar, A., Panchal, H., Prakash, N., Prasad, C., Nandakumar, S. and El Kady, M.S., 2019. Effect of water depth on a novel absorber plate of pyramid solar still coated with TiO2 nano black paint. Journal of cleaner production, 213, pp.185-191.
28. Thakur, A.K., Sathyamurthy, R., Velraj, R., Lynch, I., Saidur, R., Pandey, A.K., Sharshir, S.W., Ma, Z., GaneshKumar, P. and Kabeel, A.E., 2021. Sea-water desalination using a desalting unit integrated with a parabolic trough collector and activated carbon pellets as energy storage medium. Desalination, 516, p.115217.
29. Thakur, A.K., Sathyamurthy, R., Sharshir, S.W., Kabeel, A.E., Manokar, A.M. and Zhao, W., 2021. An experimental investigation of a water desalination unit using different microparticle-coated absorber plate: yield, thermal, economic, and environmental assessments. Environmental Science and Pollution Research, 28(28), pp.37371-37386.
30. Thakur, A.K., Sathyamurthy, R., Sharshir, S.W., Elkadeem, M.R., Ma, Z., Manokar, A.M., Arıcı, M., Pandey, A.K. and Saidur, R., 2021. Performance analysis of a modified solar still using reduced graphene oxide coated absorber plate with activated carbon pellet. Sustainable Energy Technologies and Assessments, 45, p.101046.
31. Shoeibi, S., Kargarsharifabad, H., Mirjalily, S.A.A. and Muhammad, T., 2022. Solar district heating with solar desalination using energy storage material for domestic hot water and drinking water–Environmental and economic analysis. Sustainable Energy Technologies and Assessments, 49, p.101713.
32. Shoeibi, S., Kargarsharifabad, H., Rahbar, N., Khosravi, G. and Sharifpur, M., 2022. An integrated solar desalination with evacuated tube heat pipe solar collector and new wind

ventilator external condenser. Sustainable Energy Technologies and Assessments, 50, p.101857.

33. Dhivagar, R., Mohanraj, M., Hidouri, K. and Belyayev, Y., 2021. Energy, exergy, economic and enviro-economic (4E) analysis of gravel coarse aggregate sensible heat storage-assisted single-slope solar still. Journal of Thermal Analysis and Calorimetry, 145(2), pp.475-494.
34. Thakur, A.K., Sathyamurthy, R., Velraj, R., Saidur, R., Lynch, I., Venkatesh, R., Kumar, P.G., Kim, S.C. and Sillanpää, M., 2022. A novel solar absorber using activated carbon nanoparticles synthesized from bio-waste for the performance improvement of solar desalination unit. Desalination, 527, p.115564.
35. Thakur, A.K., Sathyamurthy, R., Velraj, R., Saidur, R., Lynch, I., Chaturvedi, M. and Sharshir, S.W., 2022. Synergetic effect of absorber and condenser nano-coating on evaporation and thermal performance of solar distillation unit for clean water production. Solar Energy Materials and Solar Cells, 240, p.111698.